Journal of
Mechanical
Science and
Technology

Journal of Mechanical Science and Technology 21 (2007) 2073~2081

Transmission loss estimation of splitter silencer using multi-domain BEM

Hyeon-Don Ju[1,*], Shi-Bok Lee[2] and Young-Bum Park[3]

[1]*School of Fire & Disaster Prevention Engineering, Jinju International University, Chinju, 660-759, Korea*
[2]*School of Mechanical Engineering, Pusan National University, Pusan, 609-735, Korea*
[3]*DK Industrial Co., Ltd., 1571-16, Knock-san Industrial Complex, Songjung-Dong, Kangseo-Gu, Pusan, 618-270, Korea*

(Manuscript Received December 29, 2006; Revised August 10, 2007; Accepted August 14, 2007)

Abstract

This paper suggests a practical method, based on multi-domain BEM, to calculate the transmission loss of 3-dimensional silencers of subdomains comprised of different geometric and material characteristics with looped and/or cascaded connections. We previously proposed an efficient method to compute the transmission loss for 3-dimensional silencers using multi-domain BEM but its application is much difficult to those having looped subdomains [1]. Here, we adopt a method summing the impedance matrices of the subdomains with various types of connection represented by system graph. The algebraic overall condensed acoustic equations having only particle velocities on the subdomain interface boundaries as unknowns are formulated. A splitter silencer of cascaded, looped and symmetric connections as a sample problem is dealt with for the explanation and verification of the proposed method. An experimental work with the splitter silencer is performed to back up the suggested method.

Keywords: Transmission loss; Cascaded, Loop and symmetric connections; Multi-domain BEM(Boundary Element Method); Splitter silencer, System graph

1. Introduction

Diverse types of silencers with much different acoustic structures in the construction geometry and materials have been being used in various engineering and industrial equipments and environmental facilities [2]. Silencers of simple structure mounted already many analytical or simple approximate solutions for their acoustic behavioral characteristics. For high performance silencers of complicated structure with or without acoustic internal elements, more intricate and/or numerical analysis and design methods have been developed. But full FEM and BEM approaches to the complicated silencers result in too large variables to solve and produce the reliable analysis output even within the required analysis frequency range.

Acoustic filters and transfer matrix method [3], finite element method [4], transfer matrix method with BEM [5], multi-domain BEM(Boundary Element Method [6], BEM combining the impedance matrices for any two domains in cascaded connection [7], multi-domain structural-acoustic coupling analysis [8] may be presented as examples. Among those methods, transfer matrix method with BEM could be used to calculate relatively efficiently the transmission loss or the insertion loss of the silencer or duct systems, compared with the others. The overall transfer matrix of the whole system can be obtained by combining all the transfer matrices of the subdomains [5]. But the method has limitation in application since it is based on the assumption of plane wave propagation in the interface of subdomains, which is only true below the cutoff frequency. The global BEM algebraic equation is solved simultaneously for all of the boundary unknowns, as well as the interface variables [6]. A direct mixed-body BEM [9] was introduced to model muf-

*Corresponding author. Tel.: +82 55 751 8149, Fax.: +82 55 761 7407
E-mail address: hdju2433@hanmail.net

flers with perforated tubes, but produces a hypersingular integral and too many variables in the domains. An impedance matrix synthesis method using the direct mixed-body BEM [10] was proposed to obtain the complete impedance matrix for each subsystem separately by many different BEM runs. A sub-structuring technique combining the impedance matrices for composing sub-structures with cascaded connection using the direct mixed-body BEM was proposed [11]. The overall impedance matrix for transmission loss prediction was adopted by connecting the impedance matrices of subdomains with cascaded connection [12]. The substructure BEM was employed to predict the transmission loss of a hybrid silencer [13].

We previously proposed a practical means to formulate overall algebraic condensed equations where only particle velocities on the subdomain interface boundaries are unknowns, the solutions of which are used later to compute the overall transfer matrix elements [1]. The overall impedance matrix was assembled from all the impedance matrices of subdomains with sound pressure equilibrium and particle velocity continuity conditions at the boundaries. But it is too much difficult for the above method to deal with the complicated silencer with various types of connection. Hence we investigate a new method using system graph [14] in summing the subdomain impedance matrices to make easily the condensed overall impedance matrix for the complicated structure silencers.

For a silencer with some connected subdomains, overall acoustic linear algebraic equations condensed only with unknown particle velocities, excluding the pressure unknowns on the subdomain interface boundaries, are established. The particle velocities on the subdomain interface boundaries are used later to compute the transfer matrix elements.

If the node and element numbers of analysis models are too large, the proposed method would be too complex to manage. If the upper and lower subdomains of the silencer are symmetric with respect to longitudinal axis, the size of the impedance matrix of subdomains is simply reduced nearly by half due to the equality of particle velocities between symmetric locations.

We choose a splitter silencer as a sample problem of silencers with cascaded, loop and symmetric subdomains for verifying the proposed method, which considerably reduces the computational burden with no sacrifice of the accuracy. The impedance of perforated structures and the complex wave number and the complex density of sound absorbent materials were measured experimentally. The performance of the proposed method is validated by the transmission loss experiments.

2. Impedance matrix computation with multi-domain BEM

A body enclosed by a boundary surface can be subdivided into several domains to yield a multi-domain problem. The boundary integral formulation for the problem can be explained by considering a three dimensional enclosing boundary surface with multi-domains, Ω_I, Ω_{II}, ..., Ω_i, Ω_{i+1},..., Ω_{N-1}, Ω_N as shown in Fig. 1. It is assumed that the Ω_I and Ω_{II} are connected cascadedly and Ω_{i-1}, Ω_i, Ω_{i+1} and Ω_{i+2} are looped.

For a subdomain Ω_k, we may write a boundary integral equation as follows. The air in Ω_k is treated as compressible, inviscid and non-flowing fluid medium. For time-harmonic excitation, the velocity potential in the air satisfies the Kirchhoff-Helmholtz equation.

$$C^0(P)\Phi(P) = \int_S \{\psi(P,Q)\frac{\partial\Phi}{\partial n}(Q) - \Phi(Q)\frac{\partial\Psi}{\partial n}(P,Q)\}dS(Q) \tag{1}$$

where P is a collocation point, Q is any integration point on the boundary S and n denotes the coordinate normal to the surface. The function ψ is the three-dimensional free-domain Green's function $\psi(P,Q) = \exp[ikR(P,Q)]/R(P,Q)$, in which $R(P,Q)$ is the distance between P and Q and k is the wave number.

Similarly, for a absorbent material subdomain Ω_l, we formulate a boundary integral equation as follows. The sound absorbent material is regarded as an equivalent fluid with complex dynamic density and complex characteristic impedance. The velocity potential Φ in the absorbent material domain must satisfy the Kirchhoff-Helmholtz equation.

$$C^0(P)\Phi(P) = \int_S \{\psi(P,Q)\frac{\partial\Phi}{\partial n}(Q) - \Phi(Q)\frac{\partial\Psi}{\partial n}(P,Q)\}dS(Q) \tag{2}$$

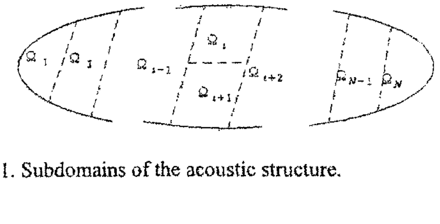

Fig. 1. Subdomains of the acoustic structure.

where $\psi(P,Q)=\exp[ik_c R(P,Q)]/R(P,Q)$, in which k_c is the complex wave constant.

The coefficient $C^o(P)$ has the value 4π for P in any domain and on any arbitrary surface can be evaluated by the following equation.

$$C^o(P) = -\int_S \frac{\partial}{\partial n}\left(\frac{1}{R(P,Q)}\right) dS(Q) \tag{3}$$

By dividing the boundary surface(including the interfaces) of Ω_k into a number of elements, the boundary integral equation can be transformed into algebraic simultaneous equations as follows:

$$\sum_{l=1}^{M} B_{jl}\cdot p_l = \sum_{l=1}^{M} A_{jk}\cdot u_l (j=1,2,\cdots,M) \tag{4a}$$

or

$$[B]\ \{p\} = [A]\{u\} \tag{4b}$$

where M represents the number of collocation points(the number of nodes on the boundary surface), l denotes the $l-th$ collocation point, j denotes the $j-th$ node on the boundary and $\{p\}$ and $\{u\}$ represent sound pressure and particle velocity vector, respectively.

Here, we rewrite Eq.(4b) as

$$\{p\} = [D]\{u\} \tag{5}$$

where the impedance matrix $[D]=[B]^{-1}[A]$ and $[B]^{-1}$ means the inverse matrix of $[B]$.

To explain the proposing method, as shown in Fig. 2, we divide the 3-dimensional enclosed structure into four domains, Ω_{inlet} , Ω_I , Ω_{II} and Ω_{outlet} . The Ω_{inlet} and Ω_{outlet} are the inlet and outlet subdomain, respectively. Ω_I and Ω_{II} represent the intermediate subdomains. And subdomains Ω_{inlet} , Ω_I , Ω_{II} and Ω_{outlet} are considered as loop connection.

The incoming velocities into Ω_{inlet} and outgoing velocities from Ω_{outlet} can be represented as follows:

$$\{u_1\} = -\{u_1^i\} \tag{6}$$

$$\{u_6\} = \{u_6^o\} \tag{7}$$

where superscripts i and o represent the inlet subdomain and the outlet subdomain, respectively and

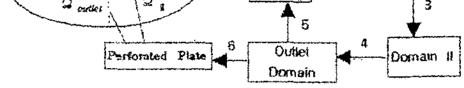

Fig. 2. Four subdomains with loop connection.

subscripts 1 and 6 represent the boundary locations as shown in Fig. 2, respectively.

Similarly, by particle velocity continuity the velocities of the interface boundaries of subdomains can be defined as follows:

$$\{u_2\} \equiv \{u_2^I\} = -\{u_2^i\} \tag{8}$$

$$\{u_3\} \equiv \{u_3^I\} = -\{u_3^{II}\} \tag{9}$$

$$\{u_4\} \equiv \{u_4^o\} = -\{u_4^{II}\} \tag{10}$$

$$\{u_5\} \equiv \{u_5^o\} = -\{u_5^i\} \tag{11}$$

If the pressures are represented as $\{p_{2+}\}\equiv\{p_2^i\}$, $\{p_{2-}\}\equiv\{p_2^I\}$, $\{p_{5+}\}\equiv\{p_5^o\}$ and $\{p_{5-}\}\equiv\{p_5^i\}$, and $[Z_{iI}]$ and $[Z_{oi}]$ of the interface boundary between Ω_{inlet} and Ω_{outlet} are given, respectively, the pressure differences at the interface boundaries are written as

$$\{p_{2+}\}-\{p_{2-}\} = -[Z_{iI}]\{u_2\} \tag{12}$$

$$\{p_{5+}\}-\{p_{5-}\} = [Z_{oi}]\{u_5\} \tag{13}$$

where i, I and o are subdomain indices and 2 and 5 represent the boundary locations as shown in Fig. 2, respectively.

Similarly, the pressures in the domains o, I and II are represented as $\{p_{4+}\}\equiv\{p_4^{II}\}$, $\{p_{4-}\}\equiv\{p_4^o\}$, $\{p_{3+}\}\equiv\{p_3^I\}$ and, $\{p_{3-}\}\equiv\{p_3^{II}\}$ and the pressure differences at the interface boundaries between Ω_{II} and Ω_{outlet} and between Ω_I and Ω_{inlet} , respectively, may be written as

$$\{p_{4+}\}-\{p_{4-}\} = [Z_{IIo}]\{u_4\} \tag{14}$$

$$\{p_{3+}\}-\{p_{3-}\} = [Z_{I\,II}]\{u_3\} \tag{15}$$

Here, we formulate Eq.(5) for Ω_{inlet} . The pressures and particle velocities at every point on the boundary of Ω_{inlet} are shown as follows:

$$\begin{bmatrix}\{p_1\}\\ \{p_{2+}\}\\ \{p_{5+}\}\end{bmatrix} = \begin{bmatrix}[D_{1,1}^i] & [D_{1,2}^i] & [D_{1,5}^i]\\ [D_{2,1}^i] & [D_{2,2}^i] & [D_{2,5}^i]\\ [D_{5,1}^i] & [D_{5,2}^i] & [D_{5,5}^i - Z_{oi}]\end{bmatrix}\begin{bmatrix}\{u_1\}\\ \{u_2\}\\ \{u_5\}\end{bmatrix} \tag{16}$$

where superscript i represents the inlet subdomain, and subscripts 1, 2 and 5 express the boundary locations 1, 2 and 5 of Ω_{inlet} shown in Fig. 2, respectively.

Similarly for Ω_I , Ω_{II} and Ω_{outlet} the relations between pressures and particle velocities at every point on the boundaries, respectively, are written as

$$\begin{bmatrix}\{p_{2-}\}\\ \{p_{3+}\}\end{bmatrix} = \begin{bmatrix}[D_{2,2}^I - Z_{iI}] & [D_{2,3}^I]\\ [D_{3,2}^I] & [D_{3,2}^I]\end{bmatrix}\begin{bmatrix}\{u_2\}\\ \{u_3\}\end{bmatrix} \tag{17}$$

$$\begin{bmatrix}\{p_{3+}\}\\ \{p_{4+}\}\end{bmatrix} = -\begin{bmatrix}[D^{II}_{3,3}-Z_{I\,II}] & [D^{II}_{3,4}]\\ [D^{II}_{4,3}] & [D^{II}_{4,4}]\end{bmatrix}\begin{bmatrix}\{u_3\}\\ \{u_4\}\end{bmatrix} \tag{18}$$

$$\begin{bmatrix}\{p_{4+}\}\\ \{p_{5+}\}\\ \{p_6\}\end{bmatrix} = \begin{bmatrix}[D^{o}_{4,4}+Z_{II\,o}] & [D^{o}_{4,5}][D^{o}_{4,6}]\\ [D^{o}_{5,4}] & [D^{o}_{5,5}][D^{o}_{5,6}]\\ [D^{o}_{6,4}] & [D^{o}_{6,5}][D^{o}_{6,6}]\end{bmatrix}\begin{bmatrix}\{u_4\}\\ \{u_5\}\\ \{u_6\}\end{bmatrix} \tag{19}$$

Eq. (16)~ Eq. (19) are assembled to formulate an overall condensed vector equation only with particle velocities on the domain interface boundaries as follows :

$$[A]\cdot\{X\}=\{B\} \tag{20}$$

where $\{X\}^T=\{\{u_2\},\{u_3\},\{u_4\},\{u_5\}\}$,

$\{B\}^T=\{-[D^{I}_{2,1}]u_1,\{0\},-[D^{o}_{4,6}]\{u_6\},-[D^{I}_{5,1}]\{u_1\}-[D^{o}_{5,6}]\{u_6\}\}$,

and $[A]$ becomes as follows:

$$\begin{bmatrix}[D^{I}_{2,2}+D^{I}_{2,2}-Z_{iI}] & [D^{I}_{2,3}] & [0] & [D^{I}_{2,5}]\\ [D^{I}_{3,2}] & [D^{I}_{3,3}+D^{II}_{3,3}-Z_{I\,II}] & [D^{II}_{3,4}] & [0]\\ [0] & [D^{II}_{4,3}] & [D^{II}_{4,4}+D^{O}_{4,4}-Z_{II\,O}] & [D^{O}_{4,5}]\\ [D^{I}_{5,2}] & [0] & [D^{0}_{5,4}] & [D^{O}_{5,5}+D^{I}_{5,5}-Z_{oi}]\end{bmatrix}$$

3. Transmission loss of the splitter silencer

Transmission loss is defined by the ratio of the inlet and outlet sound powers of the interested acoustic system. The transmission loss can be expressed as follows [9]:

$$TL=20\log_{10}\left\{\frac{1}{2}\left|T_{11}+\frac{T_{12}}{z_o}+T_{21}z_o+T_{22}\right|\right\}+10\log_{10}\frac{S_i}{S_o} \tag{21}$$

where z_o is the characteristic impedance, S_i and S_o are the cross-sectional areas of the inlet and outlet tubes, and T_{11}, T_{12}, T_{21}, and T_{22} are the four-pole parameters between the inlet and outlet of the acoustic system.

We present the procedure to determine the transmission loss of the splitter silencer shown in Fig. 3. On considering the acoustic structural characteristics of the splitter silencer, we divide the three-dimensional enclosed structure into nine subdomains, Ω_{inlet}, Ω_I, Ω_{II}, Ω_{III}, Ω_{IV}, Ω_V, Ω_{VI}, Ω_{VII}, Ω_{VIII}, Ω_{IX} and Ω_{outlet} as shown in Fig. 4. The subdomains Ω_{inlet} and Ω_{outlet} are the inlet and outlet volume, respectively. And Ω_{II}, Ω_{III}, Ω_{VI} and Ω_{VII} represent the splitter subdomains formed by two perforated guide plates and the inserted absorbent material. And Ω_I, Ω_{IV} and Ω_V represent the air

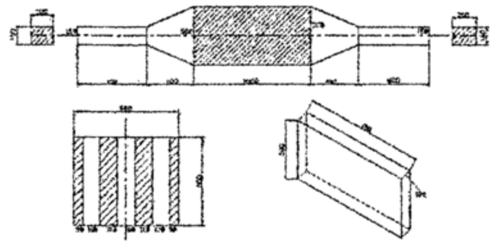

Fig. 3. Splitter silencer.

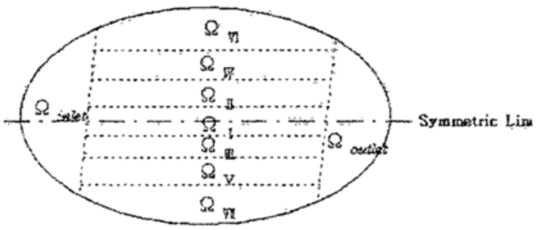

Fig. 4. Nine subdomains of the splitter silencer.

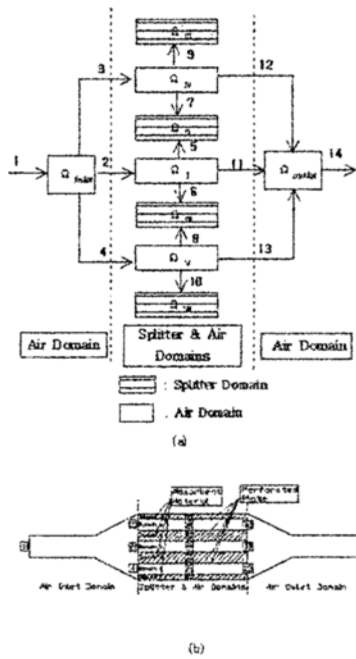

Fig. 5. Cascaded, loop and symmetric connections of nine subdomains.

subdomains. In Fig. 5, the numbers 1-14 express the boundary locations of the silencer. The upper subdomains are symmetric to the lower subdomains with respect to the longitudinal symmetric axis as shown in Fig. 4.

As shown in Fig. 5, for examples, the subdomains Ω_{inlet}, Ω_I, Ω_{II} and Ω_{VI} is regarded of loop connection and the subdomains Ω_{inlet}, Ω_l and Ω_{outlet} the cascaded connection. In this paper, the splitter silencer is adopted as the representative model with symmetric, cascaded and loop connections.

Calculation process of the four-pole parameters of the silencer is detailed in Appendix. The algebraic overall condensed acoustic equations having only particle velocities on the subdomain interface boundaries as unknowns are easily formulated by summing tables of the impedance matrices for the nine subdo mains having cascaded, loop and symmetric connections as shown in Fig. 5. The connection structure of the subdomains can be represented systematically by system graph as shown in Fig. 6.

As it is presented in Appendix A.1, Table 2(a)-2(f)

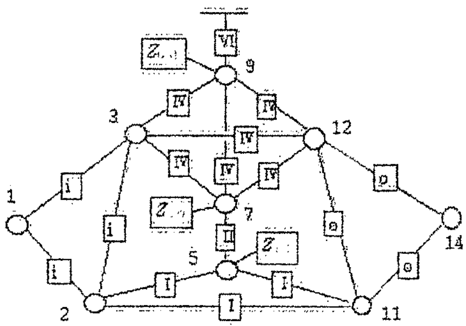

Fig. 6. System graph of the splitter silencer.

Table 1. Boundary velocities of the subdomains.

Sub-domains	Incoming Vel (1)	Outgoing Vel (1)	Incoming Vel (2)	Outgoing Vel (2)
Ω_{inlet}	$\{u_1^i\}$	$\{u_3^i\}$	$-\{u_1\}$	$-\{u_3\}$
	$\{u_1^i\}$	$\{u_2^i\}$	$-\{u_1\}$	$-\{u_2\}$
	$\{u_2^i\}$	$\{u_3^i\}$	$-\{u_2\}$	$-\{u_3\}$
Ω_l	$\{u_2^l\}$	$\{u_5^l\}$	$\{u_2\}$	$\{u_5\}$
	$\{u_2^l\}$	$\{u_{11}^l\}$	$\{u_2\}$	$\{u_{11}\}$
	$\{u_5^l\}$	$\{u_{11}^l\}$	$\{u_5\}$	$\{u_{11}\}$
Ω_{II}	$\{u_5^{II}\}$	$\{u_7^{II}\}$	$-\{u_5\}$	$-\{u_7\}$
Ω_{IV}	$\{u_3^{IV}\}$	$\{u_7^{IV}\}$	$\{u_3\}$	$\{u_7\}$
	$\{u_3^{IV}\}$	$\{u_9^{IV}\}$	$\{u_3\}$	$\{u_9\}$
	$\{u_3^{IV}\}$	$\{u_{12}^{IV}\}$	$\{u_3\}$	$\{u_{12}\}$
	$\{u_7^{IV}\}$	$\{u_9^{IV}\}$	$\{u_7\}$	$\{u_9\}$
	$\{u_7^{IV}\}$	$\{u_{12}^{IV}\}$	$\{u_7\}$	$\{u_{12}\}$
Ω_{outlet}	$\{u_{11}^o\}$	$\{u_{12}^o\}$	$-\{u_{11}\}$	$-\{u_{12}\}$
	$\{u_{11}^o\}$	$\{u_{14}^o\}$	$-\{u_{11}\}$	$-\{u_{14}\}$
	$\{u_{12}^o\}$	$\{u_{14}^o\}$	$-\{u_{12}\}$	$-\{u_{14}\}$
Ω_{III}	$\{u_5^{III}\}$		$-\{u_5\}$	
Ω_V	$\{u_4^V\}$	$\{u_{13}^V\}$	$\{u_4\}$	$\{u_{13}\}$
Ω_{VI}	$\{u_9^{VI}\}$		$-\{u_9\}$	

Table 2. Re-arranged impedance matrix elements.

(a)

	$-u_2$	$-u_3$
$u_2^i = -u_2$	$[D^i_{2,2}]$	$[2\cdot D^i_{2,3}]$
$u_3^i = -u_3$	$[D^i_{3,2}]$	$[2\cdot D^i_{3,3}]$

(b)

	u_2	u_{11}	u_5
$u_2^l = u_2$	$[D^l_{2,2}]$	$[D^l_{2,11}]$	$[2\cdot D^l_{2,5}]$
$u_{11}^l = u_{11}$	$[D^l_{11,2}]$	$[D^l_{11,11}]$	$[2\cdot D^l_{11,5}]$
$u_5^l = u_5$	$[D^l_{5,2}]$	$[D^l_{5,11}]$	$[2\cdot D^l_{5,5}]$

(c)

	$-u_5$	$-u_7$
$u_5^{II} = -u_5$	$[D^{II}_{5,5} - Z_{III}]$	$[D^{II}_{5,7}]$
$u_7^{II} = -u_7$	$[D^{II}_{7,5}]$	$[D^{II}_{7,7}]$

(d)

	u_3	u_{12}	u_7	u_9
$u_3^{IV} = u_3$	$[D^{IV}_{3,3}]$	$[D^{IV}_{3,12}]$	$[D^{IV}_{3,7}]$	$[D^{IV}_{3,9}]$
$u_{12}^{IV} = u_{12}$	$[D^{IV}_{12,3}]$	$[D^{IV}_{12,12}]$	$[D^{IV}_{12,7}]$	$[D^{IV}_{12,9}]$
$u_7^{IV} = u_7$	$[D^{IV}_{7,3}]$	$[D^{IV}_{7,12}]$	$[D^{IV}_{7,7} - Z_{V}]$	$[D^{IV}_{7,9}]$
$u_9^{IV} = u_9$	$[D^{IV}_{9,3}]$	$[D^{IV}_{9,12}]$	$[D^{IV}_{9,7}]$	$[D^{IV}_{9,9}]$

(e)

	$-u_9$
$u_9^{VI} = -u_9$	$[D^{IV}_{9,9} - Z_{VI}]$

(f)

	$-u_{11}$	$-u_{12}$
$u_{11}^o = -u_{11}$	$[D^o_{11,11}]$	$[2\cdot D^o_{11,12}]$
$u_{12}^o = -u_{12}$	$[D^o_{12,11}]$	$[2\cdot D^o_{12,12}]$

(g)

	$-u_{11}$	$-u_{12}$
$u_{11}^o = -u_{11}$	$[E^o_{11,11}]$	$[2\cdot E^o_{11,12}]$
$u_{12}^o = -u_{12}$	$[E^o_{12,11}]$	$[2\cdot E^o_{12,12}]$

Table 3. Re-arranged vector elements.

	$-u_1$	$-u_{14}$	$-p_{14}$
$u_2^i = -u_2$	$-[D^i_{2,1}]\{u_1\}$		
$u_3^i = -u_3$	$-[D^i_{3,1}]\{u_1\}$		
$u_{11}^o = -u_{11}$		$-[D^o_{11,14}]\{u_{14}\}$	$-[E^o_{11,14}]\{p_{14}\}$
$u_{12}^o = -u_{12}$		$-[D^o_{12,14}]\{u_{14}\}$	$-[E^o_{12,14}]\{p_{14}\}$

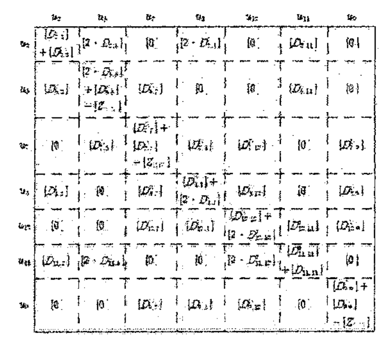

Fig. 7. The condensed matrix $[A]$ to obtain T_{12} and T_{22}.

and Table 3 are summed to build the impedance matrix $[A]$ and the vector $\{B\}$ of the overall equation, respectively as follows:

$$[A]\cdot\{X\}=\{B\} \tag{22}$$

where $\{X\}^T=\{\{u_2\},\{u_5\},\{u_7\},\{u_3\},\{u_{12}\},\{u_{11}\},\{u_9\}\}$, $\{B\}^T=\{-[D^i_{2,1}]\{u_1\},\{0\},\{0\},-[D^i_{3,1}]\{u_1\},-[D^o_{12,14}]\{u_{14}\},-[D^o_{11,14}]\{u_{14}\},\{0\}\}$, and $[A]$ is shown in Fig. 7.

The pressure vectors on the inlet boundary of Ω_{inlet} and the outlet boundary of Ω_{outlet} can be found from Eq.(A5b) and Eq.(A10), respectively, as

$$\{p_1\}=-[D^i_{1,1}]\{u_1\}-[D^i_{1,2}]\{u_2\}-[2\cdot D^i_{1,3}]\{u_3\} \tag{23}$$

$$\{p_{14}\}=-[D^o_{14,11}]\{u_{11}\}-[D^o_{14,12}]\{u_{12}\}-[D^o_{14,14}]\{u_{14}\} \tag{24}$$

Using the averaged sound pressure p_1 and the normal particle velocity u_1 at the inlet of the silencer and the averaged sound pressure p_{14} and the normal particle velocity u_{14} at the outlet, we can calculate T_{11} and T_{21} as

$$T_{11}=\frac{p_1}{p_{14}}\Big|_{u_{14}=0,u_1=1} \tag{25}$$

$$T_{21}=\frac{u_1}{p_{14}}\Big|_{u_{14}=0,\,u_1=1}=\frac{1}{p_{14}}\Big|_{u_{14}=0}. \tag{26}$$

As it is presented in Appendix A.2, Table 2(a)-2(e), Table 2(g) and Table 3 are summed to build the impedance matrix and the vector of the overall equation, respectively as follows:

$$[A]'\cdot\{X\}'=\{B\}' \tag{27}$$

where $\{X\}'^T=\{\{u_2\},\{u_5\},\{u_7\},\{u_3\},\{u_{12}\},\{u_{11}\},\{u_9\}\}$, $\{B\}'^T=\{-[D^i_{2,1}]\{u_1\},\{0\},\{0\},-[D^i_{3,1}]\{u_1\},-[E^o_{12,14}]\{p_{14}\},-[E^o_{11,14}]\{p_{14}\},\{0\}\}$, and $[A]'$ is shown in Fig. 8.

The pressure vectors on the inlet boundary of Ω_{inlet} and the outlet boundary of Ω_{outlet} can be found from Eq.(A5b) and Eq.(A11), respectively, as

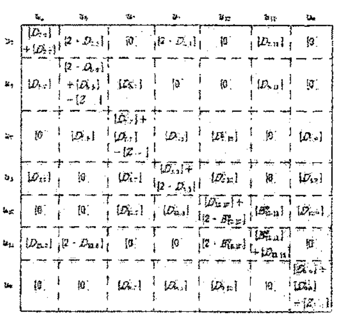

Fig. 8. The condensed matrix to obtain $[A]$ to obtain T_{12} and T_{22}.

$$\{p_1\}=-[D^i_{1,1}]\{u_1\}-[D^i_{1,2}]\{u_2\}-[2\cdot D^i_{1,3}]\{u_3\} \tag{28}$$

$$\{p_1\}=-[E^o_{14,11}]\{u_{11}\}-[2\cdot E^o_{14,12}]\{u_{12}\}-[E^o_{14,14}]\{p_{14}\} \tag{29}$$

Using the averaged sound pressure p_1 and the normal particle velocity u_1 at the inlet of the silencer and the averaged normal particle velocity u_{14} and the sound pressure p_{14} on the outlet, we compute T_{12} and T_{22} as

$$T_{12}=\frac{p_1}{u_{14}}\Big|_{p_{14}=0,u_1=1} \tag{30}$$

$$T_{22}=\frac{u_1}{u_{14}}\Big|_{p_{14}=0,u_1=1}=\frac{1}{u_{14}}\Big|_{p_{14}=0} \tag{31}$$

The four-pole parameters input into Eq.(21) yield the transmission loss of the silencer.

4. Experiments and discussion

Fig. 9 shows the schematic diagram of experimental setup for transmission loss measurements. The transmission loss of the splitter silencer is measured by the two-microphone method proposed by Seybert and Ross [15]. A random-noise generator gives the required random-noise signal, which is passed through a power-amplifier before it is fed to a horn

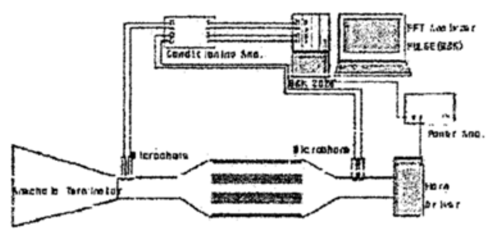

Fig. 9. Experimental setup.

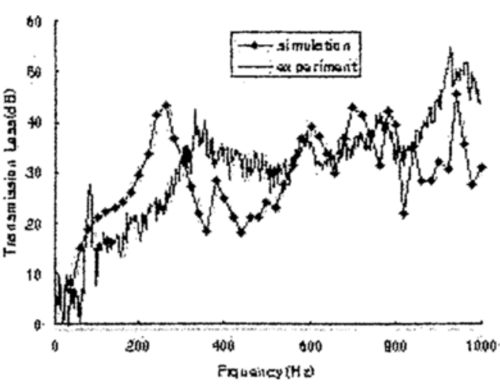

Fig. 10. Comparison of simulated and measured transmission losses.

driver, which creates an acoustic pressure field. The signal picked up by each microphone(B&K type 4188) is amplified by a conditioning amplifier, and then goes to a FFT analyzer(B&K PULSE). To collect and prepare the experimental transmission loss data, two microphones are located at the inlet and outlet of the silencer and spectral densities of signals are measured.

The test model is a splitter silencer. The dimensions of the silencer are shown in Fig. 3. The absorbent material of the splitter is glass wool and the perforated plates have the holes of 6mm diameter and the porosity of 56 %. The transfer impedances of the porous material and the perforated plates are measured directly by the transfer function method [16].

The element size of the analyzed model is decided by the consideration of the analysis range of frequency and program running time. The analyzed result approximates reasonably the experimental one as shown in Fig. 10. This confirmation experiment say that the proposed analysis program can be used as a practical means to estimate the sound transmission loss of the three dimensional silencer with internal perforated plates and absorbent materials.

5. Conclusion

This paper investigated a practical numerical analysis method to calculate the transmission loss of the splitter silencer comprised of subdomains with looped and cascaded connections. Based on multi-domain BEM, each subdomain's impedance matrix is constructed and absorbent material domains' impedance are obtained by experiments. Here, we adopt the method summing the impedance matrices of the subdomains with various types of connection represented by system graph, which gives the algebraic overall condensed acoustic equations having only particle velocities on the subdomain interface boundaries. The solutions of the overall equations are used to obtain the four pole parameters needed for computation of transmission loss. The proposed method can be applied effectively to the acoustic analysis and design of 3-dimensional silencers with complicatedly connected subdomains that doesn't allow other conventional approaches. To confirm the performance of the proposed method, comparison work of the numerically analyzed and experimental measured transmission losses was carried out and it was found that the two results coincide reasonably well.

Acknowledgement

This study was supported by Pusan National University Research Grant.

References

[1] H. D. Ju, and S. B. Lee, Transmission loss estimation of three dimensional silencers with perforated internal structures using multi-domain BEM, *Journal of Mechanical Science and Technology.* 19 (8) (2005) 1568-1575.

[2] H. D. Ju, S. B. Lee, W. B. Jeong and B. H. Lee, Design of an acoustic enclosure with duct silencers for the heavy duty diesel engine generator set, *Applied Acoustics.* 65 (2004) 441-455.

[3] M. L. Munjal, Acoustics of Ducts and Mufflers, John Wiley & Sons, New York, (1987) 75-84.

[4] R. Ramakrishnan, Design curves for rectangular splitter silencers, *Applied Acoustics.* 35 (1992) 1-24.

[5] T. Tanaka and T. Fujikawa, A method for the analytical prediction of insertion loss of a two-dimensional muffler model based on the transfer matrix derived from the boundary element method, *Journal of Vibration, Acoustics, Stress and Reliability in Design.* 107 (1985) 86-91.

[6] C. Y. R. Cheng and A. F. Seybert, A multidomain boundary element solution for silencer and muffler performance prediction, *Journal of Sound and Vibration.* 151 (1) (1991) 119-129.

[7] Z. Ji, Q. Ma and Z. Zhang, Application of the boundary element method to predicting acoustic performance of expansion chamber mufflers with mean flow, *Journal of Sound and Vibration.* 173 (1) (1994) 57-71.

[8] H. D. Ju and S. B. Lee, Multi-domain structural-acoustic coupling analysis using the finite element and boundary element techniques, *Journal of Mechanical Science and Technology.* 15 (5) (2001) 555-561.

[9] T. W. Wu, P. Zhang and C. Y. R. Cheng, Boundary element analysis of mufflers with an improved method for deriving the four-pole parameters, *Journal of Sound and Vibration.* 217 (4) (1998) 767-779.

[10] G. Lou and T. W. Wu, Impedance matrix synthesis for multiply connected exhaust network systems using the direct mixed-body BEM, *Journal of Sound and Vibration.* 238 (2) (2000) 351-362.

[11] G. Lou, T. W. Wu and C. Y. R. Cheng, Boundary element analysis of packed silencers with a substructuring technique, *Engineering Analysis with*

Boundary Elements. 27 (2003) 643-653.
[12] A. Selamet, I. J. Lee and N. T. Huff, Acoustic attenuation of hybrid silencers, *Journal of Sound and Vibration.* 262 (2003) 509-527.
[13] Z. L. Ji, Boundary element analysis of a straight-through hybrid silencer, *Journal of Sound and Vibration.* 292 (2006) 415-423.
[14] H. R. Martens and D. R. Allen, Introduction to Systems Theory, Charles E. Merrill Publishing Co., Columbus, Ohio, (1969) 131-157.
[15] A. F. Seybert and F. Ross, Experimental determination of acoustic properties using a two-microphone random excitation technique, *Journal of the Acoustical Society of America.* 61 (1977) 1362-1370.
[16] H. Utsuno, T. Tanaka, T. Fujikawa and A. F. Seybert, Transfer function method for measuring characteristic impedance and propagation constant of porous materials, *Journal of the Acoustical Society of America.* 86 (1989) 637-643.

Appendix: Intermediate calculation process for the four pole parameters

A.1 Computation of T_{11} and T_{21}

By putting the first boundary condition so that the particle velocity of the inlet of Ω_{inlet} is 1 and the particle velocity of the outlet of Ω_{outlet} is 0, T_{11} and T_{21} are calculated.

In Fig. 6, the system across variables, i.e., i, o, I, II, IV and VI, are used to express Ω_{inlet}, Ω_{outlet}, Ω_{I}, Ω_{II}, Ω_{IV} and Ω_{VI}, respectively, for convenience. The node variables 1-14 define the incoming and outgoing velocities of each subdomain element. As given in Table 1, the incoming velocities(1) and outgoing velocities(1) are equal to the incoming velocities(2) and outgoing velocities(2), respectively. The incoming and outgoing velocities(2) must have identical signs. Therefore the signs of the impedance matrix elements in the overall condensed equations become all positive. This property is extremely useful in constructing the impedance matrices in the overall equations.

By the symmetric characteristic of the splitter silencer the velocities of the interface boundary ought to satisfy following relations:

$$\{u_3\} = \{u_4\} \tag{A1a}$$

$$\{u_4\} = \{u_6\} \tag{A1b}$$

$$\{u_{12}\} = \{u_{13}\} \tag{A1c}$$

When the pressures are defined as $\{p_{5+}\} \equiv \{p_5^I\}$ and $\{p_{5-}\} \equiv \{p_5^{II}\}$, and the impedance matrix $[Z_{I\,II}]$ is given, the pressure difference can be written as follows:

$$\{p_{5+}\} - \{p_{5-}\} = [Z_{I\,II}]\{u_5\} \tag{A2}$$

Similarly, the pressures can be defined as $\{p_{7+}\} \equiv \{p_7^{II}\}$, $\{p_{7-}\} \equiv \{p_7^{IV}\}$, $\{p_{9+}\} \equiv \{p_9^{IV}\}$ and $\{p_{9-}\} \equiv \{p_9^{VI}\}$, and the pressure differences between Ω_{II} and Ω_{IV} and between Ω_{IV} and Ω_{VI} can be written, respectively as follows:

$$\{p_{7+}\} - \{p_{7-}\} = -[Z_{II\,IV}]\{u_7\} \tag{A3}$$

$$\{p_{9+}\} - \{p_{9-}\} = -[Z_{IV\,VI}]\{u_9\} \tag{A4}$$

In this case, Eq.(5) can be written for Ω_{inlet} as follows:

$$\begin{bmatrix} \{p_1\} \\ \{p_2\} \\ \{p_3\} \\ \{p_4\} \end{bmatrix} = -\begin{bmatrix} [D_{1,1}^i]\,[D_{1,2}^i]\,[D_{1,3}^i]\,[D_{1,4}^i] \\ [D_{2,1}^i]\,[D_{2,2}^i]\,[D_{2,3}^i]\,[D_{2,4}^i] \\ [D_{3,1}^i]\,[D_{3,2}^i]\,[D_{3,3}^i]\,[D_{3,4}^i] \\ [D_{4,1}^i]\,[D_{4,2}^i]\,[D_{4,3}^i]\,[D_{5,5}^i] \end{bmatrix} \begin{bmatrix} \{u_1\} \\ \{u_2\} \\ \{u_3\} \\ \{u_4\} \end{bmatrix} \tag{A5a}$$

where 1, 2, 3 and 4 express the boundary number 1, 2, 3 and 4 of Ω_{inlet} shown in Fig. 5 respectively. But in Fig. 4, as Ω_V and Ω_{VI} are symmetric with respect to the longitudinal axis, the impedance matrix of the Ω_{inlet} is simply converted by utilizing Eq.(A1a)

$$\begin{bmatrix} \{p_1\} \\ \{p_2\} \\ \{p_3\} \end{bmatrix} = -\begin{bmatrix} [D_{1,1}^i]\,[D_{1,2}^i]\,[2\cdot D_{1,3}^i] \\ [D_{2,1}^i]\,[D_{2,2}^i]\,[2\cdot D_{2,3}^i] \\ [D_{3,1}^i]\,[D_{3,2}^i]\,[2\cdot D_{3,3}^i] \end{bmatrix} \begin{bmatrix} \{u_1\} \\ \{u_2\} \\ \{u_3\} \end{bmatrix} \tag{A5b}$$

Similarly, utilizing Eq.(A1b), the relations between pressures and particle velocities at the boundary of Ω_I are given as follows:

$$\begin{bmatrix} \{p_2\} \\ \{p_{11}\} \\ \{p_{5+}\} \end{bmatrix} = -\begin{bmatrix} [D_{2,2}^I]\,[D_{2,11}^I]\,[2\cdot D_{2,5}^I] \\ [D_{11,2}^I]\,[D_{11,11}^I]\,[2\cdot D_{11,5}^I] \\ [D_{5,2}^I]\,[D_{5,11}^I]\,[2\cdot D_{5,5}^I] \end{bmatrix} \begin{bmatrix} \{u_2\} \\ \{u_{11}\} \\ \{u_5\} \end{bmatrix} \tag{A6}$$

where 2, 11 and 5 express the boundary number 2, 11 and 5 of Ω_I shown in Fig. 5, respectively.

Also, the relations between pressures and particle velocities at the boundary of Ω_{II} are written as follows:

$$\begin{bmatrix} \{p_{5+}\} \\ \{p_{7+}\} \end{bmatrix} = -\begin{bmatrix} [D_{2,2}^{II} - Z_{I\,II}] & [D_{5,7}^{II}] \\ [D_{7,5}^{II}] & [D_{7,7}^{II}] \end{bmatrix} \begin{bmatrix} \{u_5\} \\ \{u_7\} \end{bmatrix} \tag{A7}$$

where 5 and 7 express the boundary number 5 and 7 of Ω_{II} shown in Fig. 5, respectively. The pressures and particle velocities are unknown but acoustic impedance $[Z_{I\,II}]$ is measured by experiment.

And the pressures and particle velocities at the boundary of Ω_{IV} and Ω_{VI}, respectively, are shown as

$$\begin{bmatrix}\{p_3\}\\ \{p_{12}\}\\ \{p_{7+}\}\\ \{p_{9+}\}\end{bmatrix} = -\begin{bmatrix}[D^{IV}_{3,3}] & [D^{IV}_{3,12}] & [D^{IV}_{3,7}] & [D^{IV}_{3,9}]\\ [D^{IV}_{12,3}] & [D^{IV}_{12,12}] & [D^{IV}_{12,7}] & [D^{IV}_{12,9}]\\ [D^{IV}_{7,3}] & [D^{IV}_{7,12}] & [D^{IV}_{7,7}-Z_{II\,IV}] & [D^{IV}_{7,9}]\\ [D^{IV}_{9,3}] & [D^{IV}_{9,12}] & [D^{IV}_{9,7}] & [D^{IV}_{9,9}]\end{bmatrix}\begin{bmatrix}\{u_3\}\\ \{u_{12}\}\\ \{u_7\}\\ \{u_9\}\end{bmatrix} \tag{A8}$$

$$\{p_{9+}\} = -[D^{VI}_{9,9} - Z_{IV\,VI}]\{u_9\} \tag{A9}$$

Similarly, utilizing Eq.(22c), the pressures and particle velocities at the boundary of Ω_{outlet} are written as follows:

$$\begin{bmatrix}\{p_{11}\}\\ \{p_{12}\}\\ \{p_{14}\}\end{bmatrix} = -\begin{bmatrix}[D^{o}_{11,11}] & [2\cdot D^{o}_{11,12}] & [D^{o}_{11,14}]\\ [D^{o}_{12,11}] & [2\cdot D^{o}_{12,12}] & [D^{o}_{12,14}]\\ [D^{o}_{14,11}] & [2\cdot D^{o}_{14,12}] & [D^{o}_{14,14}]\end{bmatrix}\begin{bmatrix}\{u_{11}\}\\ \{u_{12}\}\\ \{u_{14}\}\end{bmatrix} \tag{A10}$$

The impedance matrix elements of Eq.(A5b)-(A10) are arranged into the elements of Table 2(a)-2(f).

In Table 4, Table 5 and Fig. 6, it is shown that the subdomains of the splitter silencer are organized by two loop connections and five cascaded connections. For example, the composition of the condensed impedance matrix, as shown in Table 4(a), of the loop connection consisted of Ω_{inlet}, Ω_I, Ω_{II} and Ω_{IV} is the same to the condensed impedance matrix of Eq.(20).

Table 2(a)-2(f) and Table 3 are summed to build the overall equation as Eq.(22).

A.2 Computation of T_{12} and T_{22}

Assuming the secondary boundary condition so that the particle velocity of the inlet of Ω_{inlet} is 1 and the sound pressure of the outlet of Ω_{outlet} is 0, T_{12} and T_{22} are calculated.

The overall acoustic equation for the nine domain system is reformulated differently from Eq.(22) as follows.

To obtain T_{12} and T_{22} among the four-pole parameters, Eq.(A10) is expressed as follows:

$$\begin{bmatrix}\{p_{11}\}\\ \{p_{12}\}\\ \{p_{14}\}\end{bmatrix} = -\begin{bmatrix}[E^{o}_{11,11}] & [2\cdot E^{o}_{11,12}] & [E^{o}_{11,14}]\\ [E^{o}_{12,11}] & [2\cdot E^{o}_{12,12}] & [E^{o}_{12,14}]\\ [E^{o}_{14,11}] & [2\cdot E^{o}_{14,12}] & [E^{o}_{14,14}]\end{bmatrix}\begin{bmatrix}\{u_{11}\}\\ \{u_{12}\}\\ \{u_{14}\}\end{bmatrix} \tag{A11}$$

Eq.(A5b)-Eq.(A9) and Eq.(A11) are arranged into Table 2(a)-2(e) and Table 2(g) and Table 3 are summed to build the overall equation as Eq.(27).

Table 4. Two subdomains of loop connection.

	u_2	u_5	u_7	u_3
u_2	$[D_{2,2}]+[D_{2,2}]$	$[2\cdot D_{2,5}]$	$[0]$	$[2\cdot D_{2,3}]$
u_5	$[D_{5,2}]$	$[2\cdot D_{5,5}]+[D_{5,5}]-[Z]$	$[D_{5,7}]$	$[0]$
u_7	$[0]$	$[D_{7,5}]$	$[D_{7,7}]+[D_{7,7}]-[Z]$	$[D_{7,3}]$
u_3	$[D_{3,2}]$	$[0]$	$[D_{3,7}]$	$[D_{3,3}]+[2\cdot D_{3,3}]$

(a)

	u_6	u_7	u_{12}	u_{11}
u_6	$[2\cdot D_{6,6}]+[D_{6,6}]-[Z]$	$[D_{6,7}]$	$[0]$	$[D_{6,11}]$
u_7	$[D_{7,6}]$	$[D_{7,7}]+[D_{7,7}]-[Z]$	$[D_{7,12}]$	$[0]$
u_{12}	$[0]$	$[D_{12,7}]$	$[D_{12,12}]+[2\cdot D_{12,12}]$	$[D_{12,11}]$
u_{11}	$[2\cdot D_{11,6}]$	$[0]$	$[2\cdot D_{11,12}]$	$[D_{11,11}]+[D_{11,11}]$

Table 5. Five subdomains of cascaded connection.

	u_2	u_{11}
u_2	$[D_{2,2}]+[D_{2,2}]$	$[D_{2,11}]$
u_{11}	$[D_{11,2}]$	$[D_{11,11}]+[D_{11,11}]$

(a)

	u_3	u_6
u_3	$[D_{3,3}]+[2\cdot D_{3,3}]$	$[D_{3,6}]$
u_6	$[D_{6,3}]$	$[D_{6,6}]+[D_{6,6}]-[Z]$

(b)

	u_3	u_{12}
u_3	$[D_{3,3}]+[2\cdot D_{3,3}]$	$[D_{3,12}]$
u_{12}	$[D_{12,3}]$	$[D_{12,12}]+[2\cdot D_{12,12}]$

(c)

	u_7	u_9
u_7	$[D_{7,7}]+[D_{7,7}]-[Z]$	$[D_{7,9}]$
u_9	$[D_{9,7}]$	$[D_{9,9}]+[D_{9,9}]-[Z]$

(d)

	u_9	u_{12}
u_9	$[D_{9,9}]+[D_{9,9}]-[Z]$	$[D_{9,12}]$
u_{12}	$[D_{12,9}]$	$[D_{12,12}]+[2\cdot D_{12,12}]$

(e)